Metamagnetism

Spin Canting and Metamagnetism in a 3D Homometallic Molecular Material Constructed by Interpenetration of Two Kinds of Cobalt(II)-Coordination-Polymer Sheets**

Ming-Hua Zeng, Wei-Xiong Zhang, Xian-Zhong Sun, and Xiao-Ming Chen

Molecular magnetism—such as ferromagnetic, ferrimagnetic, and antiferromagnetic long-range ordering properties at low temperatures—has been observed for many transition-metal complexes.[1] In contrast, only a few magnetically ordered complexes exhibit metamagnetic phase transitions,[1b,c] and most of them are heterometallic[2] or homometallic compounds[3] or metal-radical materials[4] that display low dimensionality (one- or two-dimensional structures). In particular, homometallic three-dimensional metamagnets have only been documented in several azide-bridged complexes[5] and metal phosphonates[6] or metal carboxylates.[7]

Complicated magnetic anisotropy has significant influence on the bulk magnetic properties.[8,9] Furthermore, there is a close relationship to metamagnets, which are antiferromagnets with a strong anisotropy (without a spin-flop phase) and a net magnetic moment.[9] It is well known that a pure 1D system cannot present long-range magnetic ordering at $T \neq 0$ K.[8] Only interchain interactions can lead to ordering with spontaneous magnetization, and in a 2D system long-range ordering occurs only in the Ising limit.[9] Coupling of the magnetic ordering is a consequence of the 3D structure. So far the design of polynuclear metal complexes and extended networks with predictable magnetic properties is still a challenge in the field of molecular magnetism.[1] A great deal of work is required to understand the structural factors that govern the exchange coupling between paramagnetic centers, since such a relationship is complex and so far remains elusive.[1,8]

Recently we reported synthetic approaches to homometallic coordination polymers of different dimensionalities that show weak ferromagnetic or ferrimagnetic behavior.[10] Now we have used 3-hydroxypicolinate (pico)[11] as a bischelating

[*] Dr. M.-H. Zeng, W.-X. Zhang, X.-Z. Sun, Prof. Dr. X.-M. Chen
School of Chemistry and Chemical Engineering
Sun Yat-Sen University
Guangzhou 510275 (P.R. China)
Fax: (+86) 20-8411-2245
E-mail: cescxm@zsu.edu.cn
Dr. M.-H. Zeng
Research Institute of Bioinorganic Chemistry
Department of Chemistry and Chemical Engineering
GuangXi Normal University
Guilin 541004 (P.R. China)

Supporting information for this article is available on the WWW under http://www.angewandte.org or from the author.

ligand to construct alternating chains of metal ions. Similar to phenyleneoxamate,[2a] pico should be able to mediate electronic effects between paramagnetic metal ions,[12] and may favor antiferromagnetic coupling through the *anti–anti* carboxylate bridges.[7d] Owing to the predictable lack of compensation of the individual spin moments through the bridging and asymmetrical exchanging mode of pico ligands, weakly ferromagnetic 1D chains may be created.[9,12] Employment of additional bridging 4,4′-bipyridine (4,4′-bpy) ligands can further interconnect these chains into a 2D structure, which may lead to stabilization of the magnetic ordering.[9] Clearly, the key structural or electronic characteristics control the resulting magnetic ground states and result in modulated bulk magnetic properties.[9,12] Hydrothermal treatment of Co^{II} ions and the organic ligands provided [Co$_4$(pico)$_4$(4,4′-bpy)$_3$-(H$_2$O)$_2$]$_n$·2nH$_2$O (**1**), a 3D network consisting of two different, interpenetrating 2D neutral polymers. With strong anisotropy from single ions arranged in the chains, sheets, and finally the 3D structure, **1** exhibits spin canting and typical metamagnetism.

Crystal-structure determination by X-ray crystallography showed that each of the four Co^{II} ions in the asymmetric unit of **1** is located in a distorted octahedron. Atom Co1 is coordinated by two O,N-chelating sites of two pico ligands and two 4,4′-bpy ligands, whereas Co2 is coordinated by two O,O′-chelating sites of two pico ligands and two 4,4′-bpy ligands (Figure 1, left). The two kinds of Co^{II} ions are
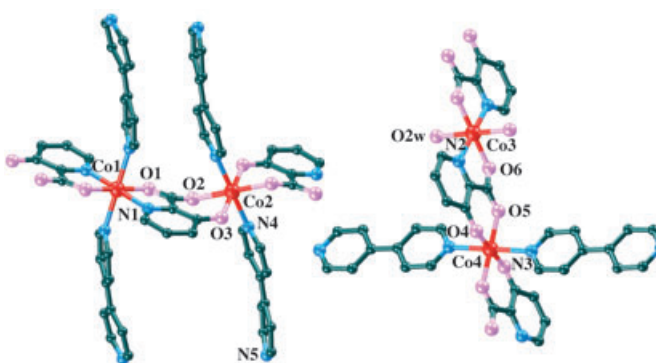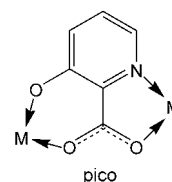

Figure 1. Perspective views of the coordination environments of Co1 and Co2 (left) and Co3 and Co4 (right) in **1**.

alternatively bridged by pico ligands to form A-type zigzag chains [Co$_2$(pico)$_2$(H$_2$O)$_2$]$_n$ (Co1···Co2 5.638(1) Å). These chains are further interlinked through 4,4′-bpy ligands into A-type sheets [Co$_2$(pico)$_2$(4,4′-bpy)(H$_2$O)$_2$]$_n$ (Co···Co 11.220(2) Å), in which the pair of pyridyl groups in each 4,4′-bpy ligand is significantly twisted with a dihedral angle of about 16° (Figure 2a). The curved conformation of the 4,4′-bpy ligands in the corrugated sheets leads to the existence of two kinds of meshes (atom–atom distance ca. 11.2 × 7.3, 11.2 × 3.5 Å).

Atom Co3 is coordinated by two pico N,O-chelating sites and two *trans* aqua ligands, whereas Co4 is coordinated by
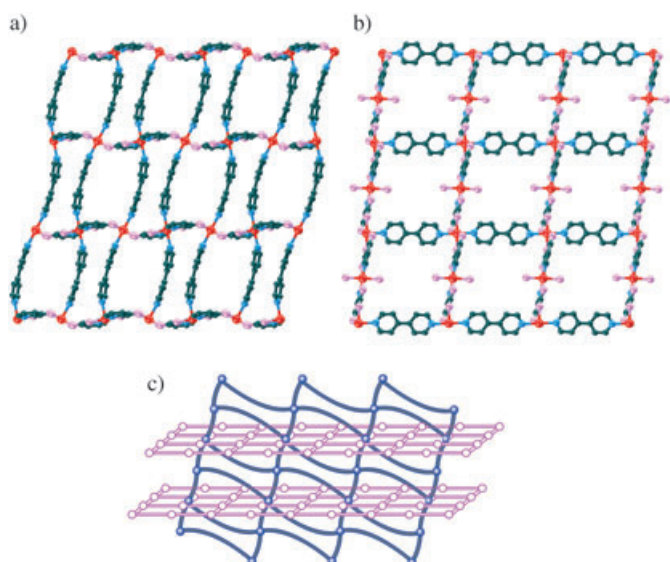
Figure 2. Views of the a) A-type and b) B-type sheets found in **1** (C green, N blue, O pink, Co red). c) A schematic representation of the interpenetrated sheets (A-type sheet blue, B-type sheet pink).

two O,O′-chelating sites of two pico ligands and two 4,4′-bpy ligands (Figure 1, right). The pico ligands alternatively bridge Co^{II} ions to form B-type zigzag chains $[Co_2(pico)_2]_n$ (Co3···Co4 5.804(1) Å), which are further bridged by the 4,4′-bpy ligands into B-type sheets $[Co_2(pico)_2(4,4′-bpy)_2]_n$ (Figure 2b; Co···Co 11.538(2) Å). This results in a square net with a uniform mesh size (atom–atom distance ca. 11.5 × 11.6 Å) different than that in the A-type sheets.

Interestingly, the two types of sheets are interpenetrated in a parallel/diagonal inclined fashion with the bigger windows of the A-type nets enclosing the 4,4′-bpy rods of the B-type nets. In addition the windows of the B-type nets contain the nodes (B chain) of the A-type nets in a 1:1 ratio.[13] This leads to a unique, compact, 3D extended network (Figure 2c and Supporting Information), featuring a strong structural anisotropy (from single-ion anisotropy to anisotropic chains, sheets, and the final 3D structure).[8, 9]

Hydrogen-bonding interactions are present between the sheets. The lattice water molecules participate in moderately strong hydrogen bonds with the pico oxygen atoms in the A-type chains (O−H···O 2.828, 3.005 Å; see Supporting Information). The aqua oxygen atoms O2w in the B-type chains form strong hydrogen bonds with the pico O2 and O3 atoms in the A-type chains of the adjacent sheets (2.711, 2.728 Å; see Supporting Information). Strong edge-to-face aromatic interactions (3.56 Å) also exist between adjacent 4,4′-bpy groups of different sheets. Although the 2D→3D parallel or inclined interpenetration of layers is not very unusual, the intertwining of different sheets is extremely rare in both inorganic and coordination polymer chemistry.[13] Complex **1** is the first example of the inclined interpenetration of two types of sheets with different composites that have the same topology (4,4-net).

The magnetic susceptibility of **1** was measured in the 2–320-K range at 100 Oe by using a polycrystalline powder sample (Figure 3a). The temperature dependence of the
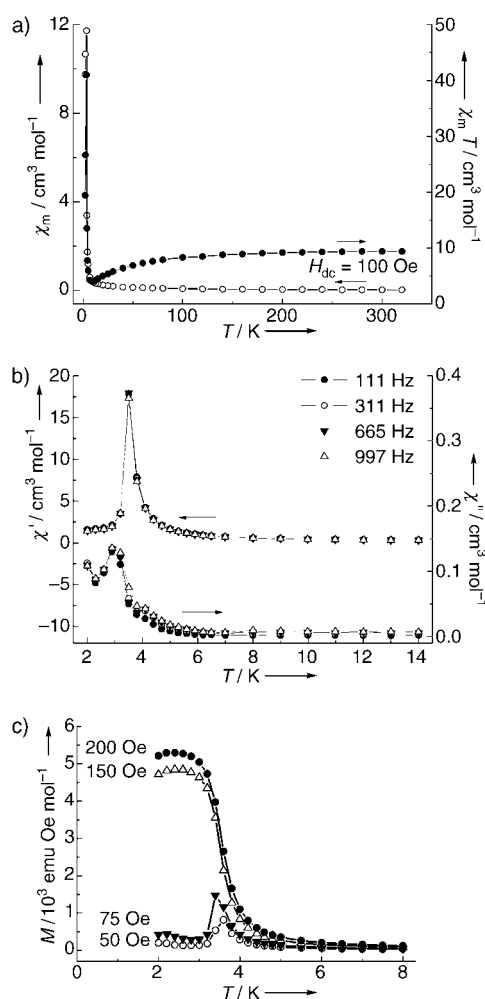

Figure 3. a) Plot of $\chi_M T$ versus T for **1**. The field strength used was $H = 100$ Oe per $\{Co^{II}\}_4$. b) The temperature dependence of the in-phase (χ') and the out-of-phase (χ'') ac magnetic susceptibilities for **1**. c) Plot of magnetization M versus T at 50, 75, 150, and 200 Oe for **1**.

reciprocal susceptibility (χ_M^{-1}) above 20 K follows the Curie–Weiss law with a Weiss constant θ of −20.4 K, thus indicating an overall strong antiferromagnetic interaction and/or spin–orbital coupling between the Co^{II} ions. The value of $\chi_M T$ at 300 K is 9.37 emu K mol⁻¹ and thus higher than the spin-only value of 7.49 emu K mol⁻¹ expected for four magnetically isolated high-spin Co^{II} ions. The product $\chi_M T$ first decreases smoothly to a rounded minimum of 4.03 emu K mol⁻¹ at 9.0 K, then increases rapidly to a very high and sharp maximum of 41.0 emu K mol⁻¹ at 3.5 K (characteristic of a magnetic long-range ordering), and finally decreases more rapidly on further cooling. The behavior above 3.5 K is characteristic of a canted antiferromagnetic chain, and that below 3.5 K may be attributed to interchain antiferromagnetic interactions and/or the saturation effect.[3]

The temperature dependence of the ac susceptibility measured in a field of 6 Oe shows the same features (Figure 3b). The maximum of χ' observed at $T_c = 3.5$ K, in agreement with the above results, confirms the occurrence of a phase transition. The absence of an out-of-phase signal (χ'') at this temperature points to a long-range antiferromagnetic

order. However, the imaginary component χ'' presents a peak at 3.0 K, which is the signature of a magnetized state, thus indicating that a partly canted antiferromagnetic structure exists below this temperature.[7a] No frequency dependence of these transitions is observed.

The temperature dependence of the magnetization of **1** at various fields is shown in Figure 3c. For applied fields below 100 Oe, the field-cooled (FC) curves present a maximum at 3.5 K, thus indicating that some interlayer antiferromagnetic interactions are operative. However, a magnetic field above 150 Oe is sufficient to overcome these weak interactions, and **1** presents a field-induced transition from an antiferromagnetic to a ferromagnetic-like state.[2–4,9] The magnetization was also measured in the range of 2–30 K (see Supporting Information). The field-cooled magnetization (FCM), measured under an applied field of 10 G, increases rapidly on cooling to 3.5 K and then diminishes. The zero-field-cooled magnetization (ZFCM) shows a maximum at 3.5 K and decreases rapidly as the temperature is further increased. This behavior implies metamagnetic ordering.[2–4,9]

Interestingly, in the $M–H$ curve of **1** around the transition temperatures and magnetic hysteresis (Figure 4a), the mag-
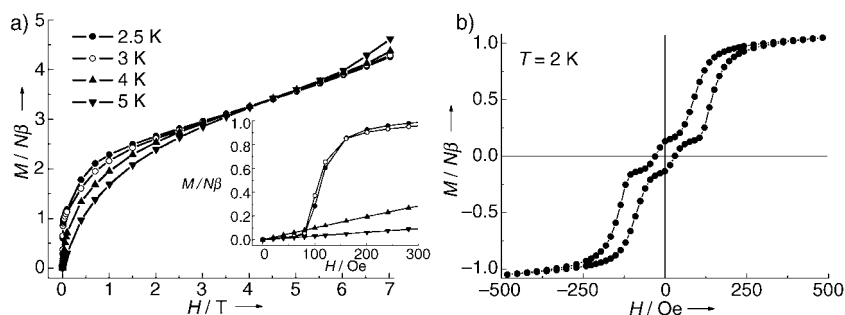

Figure 4. Plots of a) the first magnetization at 2–5 K (the inset shows the detail in a low field (0–300 Oe) at 2–5 K) and b) the hysteresis loop at 2 K.

netization curves for different temperatures below the transition temperature exhibit a sigmoidal shape with a common crossing point for $H = 160$ Oe; the 2.5-K isotherm indicates clearly that the saturation is not reached even with 70 kOe ($M = 4.35\,N\mu_B$; N = Avogadro number, μ_B = Bohr magneton). The low-field magnetization presents a small butterfly-shaped hysteresis with a metamagnetic-like transition around 160 Oe (Figure 4b), in agreement with the *FC* results. All these facts clearly confirm a metamagnetic behavior of **1** with a critical temperature T_c of 3.5 K and a critical field H_c of about 160 Oe. This reversal involves an increase of around $0.8\,\mu_B$ per Co$_4$ unit.

All the structural factors in **1** diminish the antiferromagnetic interaction to a greater extent to favor the ferromagnetic interaction observed.[9] The magneto–structural correlation indicates that there exists a strong structural anisotropy in **1** and, consequently, anisotropy in competitions between the exchange interactions of the 3D motif, which result in a typical metamagnetism. The antiferromagnetic interactions operate between Co^{II} ions of adjacent sheets, possibly through electrostatic (dipolar) interactions and hydrogen bonding

between the interpenetrated adjacent sheets.[3,13] The reason why the transition fields are so low in **1** is not yet clear, but the contribution of the substantial hydrogen bonding and dipolar interaction between the interpenetrated sheets and of the conjugated bridging ligands, as well as spin canting in the crystal lattice, may play a role in this phenomenon.[3,4,8]

In conclusion, the bridging pico ligand can be used to prepare a molecular-based magnetic material constructed by unusual interpenetration of two types of coordination sheets, which leads to a beautiful low-field metamagnetic transition and spin-canted behavior. This work demonstrates the importance of the crystal engineering of coordination polymers in the field of molecular-based magnetic materials.

Experimental Section

[1] a) E. Coronado, F. Palacio, J. Veciana, *Angew. Chem.* **2003**, *115*, 2674–2676; *Angew. Chem. Int. Ed.* **2003**, *42*, 2570–2572; b) C. Janiak, *Dalton Trans.* **2003**, 2781–2804; c) "Metal-Organic and

Organic Molecular Magnets": P. Day, A. E. Underhill, *Philos. Trans. R. Soc. London Ser. A* **1999**, *357*, 2849–3184.

[2] a) C. L. M. Pereira, E. F. Pedroso, H. O. Stumpf, M. A. Novak, L. Ricard, R. Ruiz-García, E. Rivière, Y. Journaux, *Angew. Chem.* **2004**, *116*, 974–976; *Angew. Chem. Int. Ed.* **2004**, *43*, 956–958; b) Y.-Z. Zhang, S. Gao, H.-L. Sun, G. Su, Z.-M. Wang, S.-W. Zhang, *Chem. Commun.* **2004**, 1906–1907; c) S. Ohkoshi, Y. Arimoto, T. Hozumi, H. Seino, Y. Mizobe, K. Hashimoto, *Chem. Commun.* **2003**, 2772–2773.

[3] a) E.-Q. Gao, Y.-F. Yue, S.-Q. Bai, Z. He, C.-H. Yan, *J. Am. Chem. Soc.* **2004**, *126*, 1419–1429; b) L.-M. Zheng, S. Gao, H.-H. Song, S. Decurtins, A. J. Jacobson, X.-Q. Xin, *Chem. Mater.* **2002**, *14*, 3143–3147; c) P. S. Mukherjee, S. Dalai, E. Zangrando, F. Lloret, N. R. Chaudhuri, *Chem. Commun.* **2001**, 1444–1445; d) X. Hao, Y.-G. Wei, S.-W. Zhang, *Chem. Commun.* **2000**, 2271–2272; e) M. Monfort, I. Resino, J. Ribas, H. Stoeckli-Evans, *Angew. Chem.* **2000**, *112*, 197–199; *Angew. Chem. Int. Ed.* **2000**, *39*, 191–193.

[4] a) H. Kumagai, K. Inoue, *Angew. Chem.* **1999**, *111*, 1694–1696; *Angew. Chem. Int. Ed.* **1999**, *38*, 1601–1603; b) C. Aoki, T. Ishida, T. Nogami, *Inorg. Chem.* **2003**, *42*, 7616–7625.

[5] E.-Q. Gao, Z.-M. Wang, C.-H. Yan, *Chem. Commun.* **2003**, 1748–1749.

[6] a) P. Yin, L.-M. Zheng, S. Gao, X.-Q. Xin, *Chem. Commun.* **2001**, 2346–2347; b) W.-K. Chang, R.-K. Chiang, Y.-C. Jiang, S.-L. Wang, S.-F. Lee, K.-H. Lii, *Inorg. Chem.* **2004**, *43*, 2564–2568.

[7] a) Z.-L. Huang, M. Drillon, N. Masciocchi, A. Sironi, J.-T. Zhao, P. Rabu, P. Panissod, *Chem. Mater.* **2000**, *12*, 2805–2812; b) H. Kumagai, C. J. Kepert, M. Kurmoo, *Inorg. Chem.* **2002**, *41*, 3410–3422; c) R.-H. Wang, E.-Q. Gao, M.-C. Hong, S. Gao, J.-H. Luo, Z.-Z. Lin, L. Han, R. Cao, *Inorg. Chem.* **2003**, *42*, 5486–5488; d) T.-F. Liu, H.-L. Sun, S. Gao, S.-W. Zhang, T.-C. Lau, *Inorg. Chem.* **2003**, *42*, 4792–4794.

[8] O. Kahn, *Molecular Magnetism*, VCH, New York, **1993**.

[9] a) J.-P. Renard in *Organic and Inorganic Low Dimensional Crystalline Materials* (Eds.: M. Drillon, P. Delhaes), Plenum, New York, **1987**, p. 125; b) R. L. Carlin, *Magnetochemistry*, Springer, Berlin, **1986**.

[10] a) H.-J. Chen, Z.-W. Mao, S. Gao, X.-M. Chen, *Chem. Commun.* **2001**, 2320–2321; b) M.-H. Zeng, S. Gao, X.-L. Yu, X.-M. Chen, *New J. Chem.* **2003**, *27*, 1599–1602; c) M.-H. Zeng, S. Gao, X.-M. Chen, *Inorg. Chem. Commun.* **2004**, *7*, 864–867.

[11] S. M. O. Quintal, H. I. S. Nogueira, V. Félix, M. G. B. Drew, *New J. Chem.* **2000**, *24*, 511–517.

[12] a) K. Itoh, M. Minoshita, *Molecular Magnetism, New Magnetic Materials*, Gordon Breach-Kodansha, Tokyo, **2000**; b) J. B. Goodenough, *Magnetism and the Chemical Bond*, Wiley, New York, **1963**.

[13] B. Moulton, M. J. Zaworotko, *Chem. Rev.* **2001**, *101*, 1629–1658, and references therein; b) S. R. Batten, R. Robson, *Angew. Chem.* **1998**, *110*, 1558–1595; *Angew. Chem. Int. Ed.* **1998**, *37*, 1460–1494; c) M. J. Zaworotko, *Chem. Commun.* **2001**, 1–9; d) S. R. Batten, *CrystEngComm* **2001**, *18*, 1–7; e) L. Carlucci, G. Ciani, D. M. Proserpio, *New J. Chem.* **1998**, *22*, 1319–1321.

[14] SHELXTL 6.10, Bruker Analytical Instrumentation, Madison, Wisconsin, USA, **2000**.

[15] O. V. Dolomanov, A. J. Blake, N. R. Champness, M. Schroder, *J. Appl. Crystallogr.* **2003**, *36*, 1283–1284.